Mon. Not. R. Astron. Soc. **333,** 952–960 (2002)

Short-period line profile and light variations in the Beta Cephei star 19 Monocerotis

L. A. Balona,[★1] D. J. James,[2,3] P. Motsoasele,[4] B. Nombexeza,[5] A. Ramnath[6] and J. van Dyk[7]

[1]*South African Astronomical Observatory, PO Box 9, Observatory 7935, Cape Town, South Africa*
[2]*School of Physics and Astronomy, University of St Andrews, St Andrews*
[3]*Observatoire de Genève, Chemin des Maillettes, no 51, CH-1290 Sauverny, Switzerland*
[4]*University of Cape Town, Private Bag, Rondebosch 7701, South Africa*
[5]*University of Fort Hare, Private Bag X1314, Alice 5700, South Africa*
[6]*University of the Witwatersrand, Private Bag 3, WITS, 2050, South Africa*
[7]*University of Pretoria, Pretoria 0002, South Africa*

Accepted 2002 March 11. Received 2002 January 24

ABSTRACT

We present an analysis of 555 high-dispersion echelle spectra of 19 Mon obtained from two sites as well as 115 Strömgren *uvby* observations. We show that three periodicities are present at 5.229 94, 0.170 19 and 4.889 56 cycle d^{-1}. The first periodicity has by far the largest amplitude. Photometric amplitude ratios and phase differences indicate an $\ell = 2$ mode, while the line profile variations unequivocally point to $\ell = 2, m = -2$. Because of the low amplitudes of the other two modes, very little can be said concerning them. Although 19 Mon was originally selected on the basis of its classification as a marginal Be star, the Be nature of the star is not supported by our observations.

Key words: stars: emission-line, Be – stars: individual: β Cephei – stars: individual: 19 Mon – stars: oscillations.

1 INTRODUCTION

Irvine (1975) noted very weak emission in Hα for the B1V star 19 Mon (HR 2648, HD 52918) during 1973 March. The emission nature of the star was confirmed by Hirata & Asada (1976) who found Hα absorption to be weaker than expected for a normal B1V star in 1975 November. Also very weak red emission and a weak central absorption (shell) feature seem to be present. These are the only two references in which line emission is mentioned.

The star was discovered to be a β Cep variable by Balona (1977). Balona & Engelbrecht (1979) were able to detect two frequencies at $\nu_0 = 5.2301$ and 5.0659 cycle d^{-1} in the light variation. Balona, Cuypers & Marang (1992) confirmed the presence of ν_0, but were unable to detect the secondary period. A periodicity with $\nu_1 = 0.17$ cycle d^{-1} and a possible, very weak periodicity at $\nu_2 = 4.9$ cycle d^{-1} were also detected. Heynderickx (1992) was able to confirm ν_0, but no other periodicity was clearly present in his Walraven photometry. However, a possible secondary frequency of 5.2826 cycle d^{-1} may be present in the ultraviolet band, but the 1 cycle d^{-1} alias is particularly severe. Heynderickx, Waelkens & Smeyers (1994) were able to identify ν_0 as a pulsation with spherical harmonic degree $\ell = 2$ using amplitude ratios, while the 5.2826 cycle d^{-1} periodicity appears to be a radial mode.

Many Be stars are known to be photometric and line profile variables with periods in the range 0.5–2.0 d. The period is consistent with the rotational period of the star (Balona 1990, 1995). The periodicity may offer a clue to the unknown mass-loss mechanism, which results in an equatorial disc of circumstellar material. Apart from 19 Mon, only one other Be star, 27 CMa, is known to be a β Cep star (Balona & Rozowsky 1991; Balona & Krisciunas 1994). A few Be stars appear to pulsate with modes of high degree and periods similar to those of the β Cep stars. These high-degree modes do not, in general, lead to measurable photometric variations. Nevertheless, the physical phenomenon is the same and by extending the definition, they may also be considered to be β Cep variables.

The presence of β Cep pulsations in a Be star is unusual and interesting. As a result, we observed the star with a high-resolution echelle spectrograph and simultaneous Strömgren photometry at the South African Astronomical Observatory (SAAO) for two consecutive weeks in 2001 January. During the same period, high-resolution echelle spectroscopy of 19 Mon was obtained at the Mount Stromlo and Siding Spring Observatory (MSSSO). In this paper we analyse these data and discuss the nature of 19 Mon.

★E-mail: lab@saao.ac.za

Table 1. Observing log for the spectroscopy at SAAO and MSSSO. For each observatory, the Julian day, with respect to JD 245 1900, is shown for the first and last spectrum of 19 Mon on the given night. *N* is the number of spectra obtained on that night.

SAAO			MSSSO		
Start	End	*N*	Start	End	*N*
13.32	13.60	35	13.98	14.17	7
14.29	14.60	38	15.00	15.13	9
15.29	15.61	40	15.96	16.15	9
16.31	16.61	36	17.18	17.25	6
17.29	17.60	40	18.09	18.24	11
18.29	18.61	41	18.95	19.17	10
19.29	19.61	41	19.96	20.24	24
20.54	20.62	11	20.96	21.25	29
21.29	21.61	41	21.97	22.18	9
22.32	22.34	4	22.95	22.98	4
23.29	23.60	8	24.02	24.23	21
24.29	24.61	41			
25.29	25.60	40			

Table 2. Projected rotational velocity, $v \sin i$ ($\mathrm{km\,s^{-1}}$) obtained by the non-linear least-squares method for various lines (laboratory wavelengths given). The standard deviation of the fit, σ, is in continuum units. The column labelled RV is the radial velocity of the line ($\mathrm{km\,s^{-1}}$) as obtained from the fit.

Line	$v \sin i$	σ	RV
SAAO:			
He I 4387.929	261	0.0013	35.6
He I 4471.682	273	0.0015	38.8
Si III 4552.622	282	0.0025	37.4
He I 4713.376	287	0.0017	62.1
He I 4921.931	275	0.0017	55.0
He I 5015.678	269	0.0024	32.1
He I 5875.966	266	0.0085	39.9
He I 6678.151	276	0.0016	39.0
SAAO all lines	274 ± 3		
MSSSO:			
He I 4921.931	281	0.0034	53.9
He I 5015.678	275	0.0032	50.8
He I 6678.151	270	0.0032	35.7
MSSSO all lines	275 ± 3		

2 OBSERVATIONS

Spectroscopic observations at SAAO were obtained using the GIRAFFE echelle fibre-fed spectrograph attached to the Cassegrain focus of the 1.9-m telescope. The GIRAFFE spectrograph has a resolving power of about 32 000. The 1024×1024 TEK charge-coupled device (CCD) chip gives a dispersion of $0.06–0.09$ Å $\mathrm{pixel^{-1}}$. A Th–Ar arc lamp was used for wavelength calibration with arc spectra taken at regular intervals to calibrate possible drifts. Flat-fielding was accomplished by illuminating the camera with uniform light using a tungsten filament lamp and a diffusing screen. The blaze correction was determined by measuring the response across each order when the fibre was illuminated by a tungsten lamp. The wavelength range was 4400–6680 Å spread over 45 orders. Exposure times were normally 10 min for a signal-to-noise (S/N) ratio of about 150. A total of 416 spectra of 19 Mon was obtained (Table 1) over a consecutive 2-week period in 2001 January 3–15.

The spectroscopic observations made at the Mount Stromlo and Siding Spring observatory were obtained with the coudé echelle spectrograph on the Mount Stromlo 1.9-m telescope during the same period. The observations were performed with a 31 line $\mathrm{mm^{-1}}$ echelle grating, a 2048×4096 pixel TEK CCD and a 1.2-arcsec slit, yielding a resolving power of about 40 000. The wavelength range obtained with this set-up was 4930–6750 Å, spread over 32 orders. Exposure times were nominally 10–15 min for a S/N ratio of about 100. A Th–Ar arc lamp was used for wavelength calibration with arc spectra taken at regular intervals to calibrate possible drifts. Flat-fielding was accomplished by illuminating the camera with uniform light using a tungsten filament lamp. A total of 139 spectra of 19 Mon was obtained (Table 1).

In order to study the line profile variations, the continuum needs to be determined. Placing the continuum by hand is not an easy process. We preferred to rectify the spectra with the aid of a synthetic spectrum calculated using the SPECTRUM code (Gray & Corbally 1994) using a Kurucz solar-abundance model atmosphere appropriate to a B1V star ($T_{\rm eff} = 24\,000$, $\log g = 3.50$) and broadened with $v \sin i = 270\,\mathrm{km\,s^{-1}}$. Results are insensitive to temperature, gravity or projected rotational velocity.

Strömgren *uvby* photometry was obtained using the Modular Photometer attached to the 0.5-m reflector of the SAAO simultaneously with the echelle data at the same site. We used two local comparison stars, HR 2521 and HR 2624. All three stars were observed in sequence. A total of 115 *uvby* data points were obtained during 9 nights. Analyses showed that HR 2521 appears to be slightly variable with a frequency of 1.6 or 2.6 cycle $\mathrm{d^{-1}}$. Therefore, we made use only of HR 2624 as a comparison for which we assumed the following values: $y = 5.951$, $b = 5.934$, $v = 6.014$, $u = 6.977$.

3 PHYSICAL PARAMETERS

The projected rotational velocity of 19 Mon is given as $v \sin i = 350\,\mathrm{km\,s^{-1}}$ by Slettebak & Howard (1955), and $v \sin i = 270\,\mathrm{km\,s^{-1}}$ by Slettebak (1982). We determined $v \sin i$ from various helium and metal lines using the intrinsic line profile calculated from the SPECTRUM program and a non-linear least-squares optimizing algorithm, leaving the radial velocity as a free parameter. Results are given in Table 2 and fits to the SAAO spectra shown in Fig. 1. We obtain $v \sin i = 274 \pm 3\,\mathrm{km\,s^{-1}}$ from the He I lines and the Si III 4553 line in the SAAO spectra. This is in excellent agreement with the values obtained from the MSSSO spectra (Table 2) and also with the result of Slettebak (1982).

The *Hipparcos* parallax of 19 Mon is 2.92 ± 0.87 mas. The uncertainty is too large to give a useful parallax, which would be helpful in determining the luminosity. The equivalent width (EW) of the Hγ line from our spectra is $W_\gamma = 3.56 \pm 0.01$ Å, which leads to an absolute magnitude $M_V = -3.8 \pm 0.4$ from Balona & Crampton (1974). The mean Strömgren β index ($\beta = 2.591$) gives $M_V = -3.87$ (Balona & Shobbrook 1984). The calibration of Balona (1994) gives $\log T_{\rm eff} = 4.41 \pm 0.05$ ($T_{\rm eff} = 25\,500$ K), $\log g = 4.0 \pm 0.5$ from the mean *uvby* indices. From these data we find $\log L/\mathrm{L_\odot} = 4.5 \pm 0.2$ and a radius $r = 9 \pm 3\,\mathrm{R_\odot}$. Evolutionary tracks using the Warsaw–New Jersey evolutionary code gives a mass of $M = 14 \pm 2\,\mathrm{M_\odot}$. From this, we estimate that the longest period of rotation is

about 1.6 ± 0.5 d. The critical velocity of rotation is about $560 \pm 130\,\mathrm{km\,s^{-1}}$, from which we estimate the minimum period of rotation to be 0.8 ± 0.4 d and the angle of inclination to be greater than 30°.

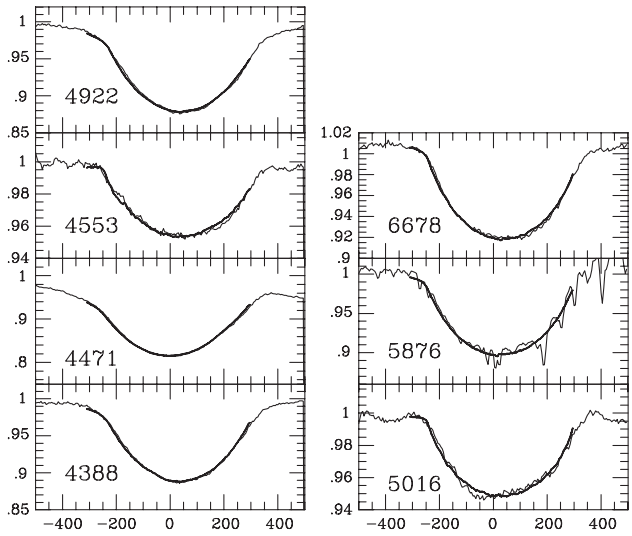

Figure 1. Mean rectified profiles of some He I lines and the Si III 4553 line in 19 Mon. The best model fit for projected rotational velocity is shown by the heavy line and covers the range of the fit. The abscissa is in units of $\mathrm{km\,s^{-1}}$ as measured from the laboratory wavelength of the line.

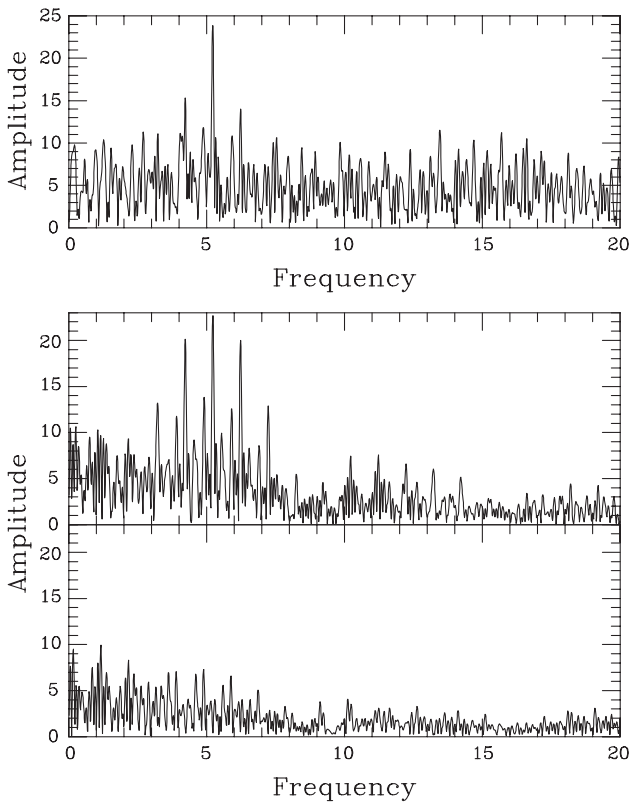

Figure 2. Fourier periodograms of He I 4922 radial velocities obtained at SAAO and MSSSO (top figure) and Strömgren *b* photometry obtained at SAAO (bottom figure) obtained in 2001 January. The top panel of the bottom figure shows the periodogram of the original data and the bottom panel the periodogram after pre-whitening for $\nu_0 = 5.23\,\mathrm{cycle\,d^{-1}}$. The frequency is in $\mathrm{cycle\,d^{-1}}$. The amplitude is in $\mathrm{km\,s^{-1}}$ and mmag in the top and bottom figures, respectively.

4 PERIOD ANALYSES

In Fig. 2 we show the periodograms of our 2001 January Strömgren *b*-band photometry. The highest peak occurs at $\nu_0 = 5.23 \pm 0.01\,\mathrm{cycle\,d^{-1}}$. Pre-whitening by ν_0 does not lead to any other significant periodicity, the highest peak being at $1.16\,\mathrm{cycle\,d^{-1}}$, which could be the 1 day alias of the $0.17\,\mathrm{cycle\,d^{-1}}$ found by Balona et al. (1992). There is no sign of a secondary frequency close to ν_0 as detected by Balona & Engelbrecht (1979) or the secondary frequency at $5.2826\,\mathrm{cycle\,d^{-1}}$ suggested by Heynderickx (1992).

A periodogram of *Hipparcos* photometry shows ν_0 very clearly. Pre-whitening by ν_0 leads to a noise spectrum. We combined the *Hipparcos* data with our 2001 Strömgren *b* photometry and the 1987 data of Balona et al. (1992) and calculated the periodogram (Fig. 3), from which we obtain $\nu_0 = 5.229\,94\,\mathrm{cycle\,d^{-1}}$. These data, when pre-whitened by ν_0, leads to a significant periodicity at $\nu_1 = 0.170\,19\,\mathrm{cycle\,d^{-1}}$. Pre-whitening by ν_0 and ν_1 shows a further significant periodicity at $\nu_2 = 4.889\,56\,\mathrm{cycle\,d^{-1}}$. Periodograms are shown in Fig. 3. We conclude that apart from ν_0, there are two additional periods in the light variations that are not significant in the individual data sets, but become so when the data sets are combined. The two additional periods, ν_1 and ν_2, are the same as those found by Balona et al. (1992). We cannot confirm the $5.2826\,\mathrm{cycle\,d^{-1}}$ periodicity that Heynderickx (1992) suspected to exist. Note that there is a relationship $\nu_0 - \nu_2 = 2\nu_1$, which is either coincidence or suggests some kind of non-linear interaction.

We measured the radial velocities by finding the position of maximum absorption in the line. An alternative method would be to find the centroid of the line, but this leads to a lower amplitude and is less useful for the purposes of finding the periods. The

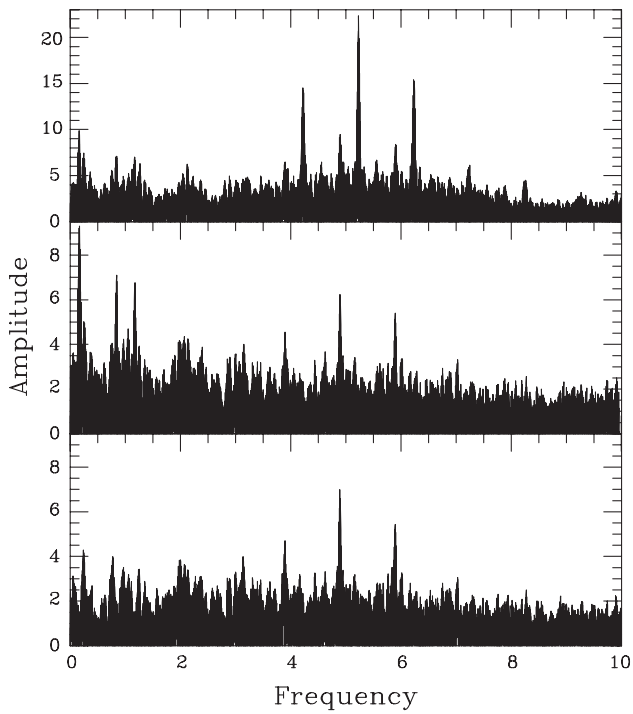

Figure 3. Fourier periodograms of the combined 1987 *Hipparcos* and 2001 photometry (top panel). In the middle panel, the data were pre-whitened by $\nu_0 = 5.22994\,\mathrm{cycle\,d^{-1}}$ and in the bottom panel by ν_0 and $\nu_1 = 0.17019\,\mathrm{cycle\,d^{-1}}$. The highest peak in the bottom panel occurs at $\nu_2 = 4.88956\,\mathrm{cycle\,d^{-1}}$. The frequency is in $\mathrm{cycle\,d^{-1}}$. The amplitude is in mmag.

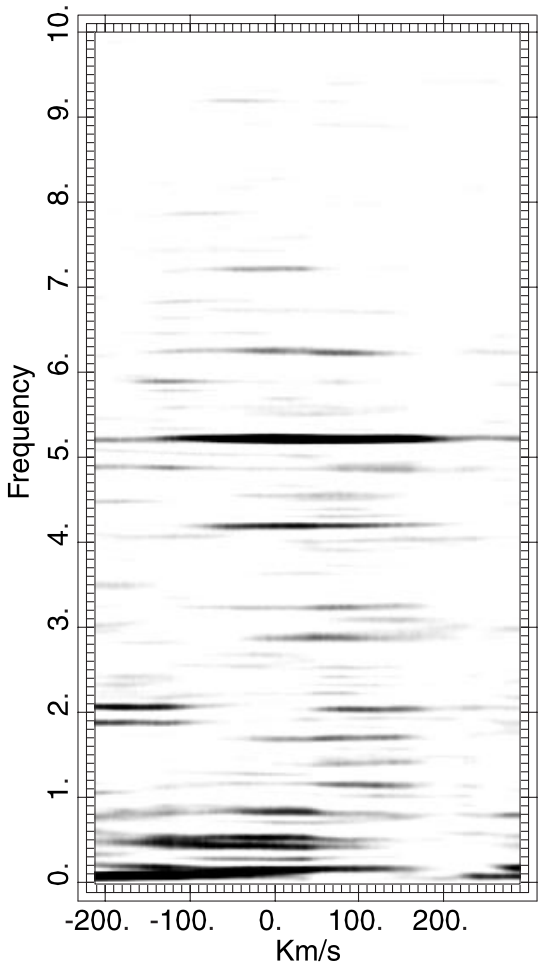

Figure 4. Grey-scale plots of power spectra across the correlation profile for the combined SAAO and MSSSO spectra.

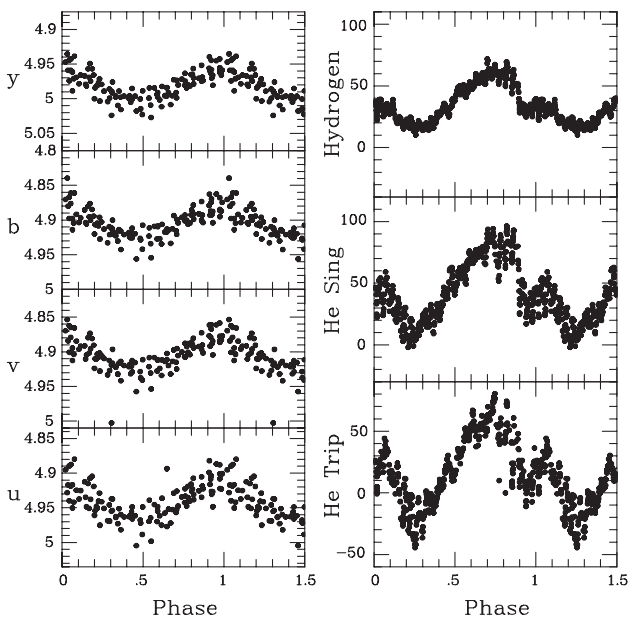

Figure 5. Left-hand panel: Strömgren *uvby* light curves of 19 Mon phased with $\nu_0 = 5.23\,\mathrm{cycle\,d^{-1}}$. Right-hand panel: velocity curves of helium triplets, helium singlets and the hydrogen lines. The epoch of phase zero is the time of light maximum at HJD 245 1900.0840.

periodogram of the radial velocities of the He I 4922 line from the SAAO and MSSSO observations is shown in Fig. 2. Again, the only significant periodicity is $\nu_0 = 5.20\,\mathrm{cycle\,d^{-1}}$. The same is true for the radial velocities of all other measured lines.

The radial velocity only samples the core of the line profile and may not be a good indicator of periodicities if the variations happen to have a small amplitude in the centre of the line profile. One common method of determining frequencies from spectroscopic data is to calculate the periodogram at each wavelength across the line profile. In Fig. 4 we show a grey-scale plot of such a diagram for the correlation profiles of the combined SAAO and MSSSO data. Apart from ν_0, there is power at low frequencies as well. We see $\nu_1 = 0.170\,19\,\mathrm{cycle\,d^{-1}}$ and also power at the $1\,\mathrm{cycle\,d^{-1}}$ aliases at 0.83 and $1.17\,\mathrm{cycle\,d^{-1}}$. Pre-whitening by ν_1 removes all power at low frequencies. The frequency $\nu_2 = 4.889\,56\,\mathrm{cycle\,d^{-1}}$ is also weakly present in Fig. 4. This shows that ν_1 and ν_2 are present in the line profiles, even though they do not have significant amplitudes in the core radial velocities.

In Fig. 5 we show the light curves phased with $\nu_0 = 5.229\,94\,\mathrm{cycle\,d^{-1}}$ in all four passbands and also the radial velocity curves of the helium triplets, singlets and hydrogen lines. The phases are relative to the epoch of maximum light (*y* band) at HJD 245 1900.0840. As individual radial velocities have large errors because the lines are very broad, the plots show a running mean of the velocities over five consecutive data points. Amplitudes and phase differences for the light and radial velocities for ν_0 are listed in Table 3.

By removing the variations of the other two periods, it is possible to extract the light and radial velocity curves for the third period. In Fig. 6 we show the light and radial velocity curves

Table 3. Amplitudes and phase differences with respect to maximum *y* light for the $\nu_0 = 5.23\,\mathrm{cycle\,d^{-1}}$ periodicity. Amplitudes are in mmag and $\mathrm{km\,s^{-1}}$ and phases are in radians.

Band	Amplitude	$\phi - \phi_y$
y	23.7 ± 1.5	0.00 ± 0.06
b	23.4 ± 1.7	0.00 ± 0.07
v	25.7 ± 2.0	0.10 ± 0.08
u	28.0 ± 2.3	0.07 ± 0.08
He triplets	32.6 ± 2.9	4.71 ± 0.09
He singlets	31.4 ± 2.4	4.73 ± 0.08
Hydrogen	20.4 ± 1.2	4.71 ± 0.06

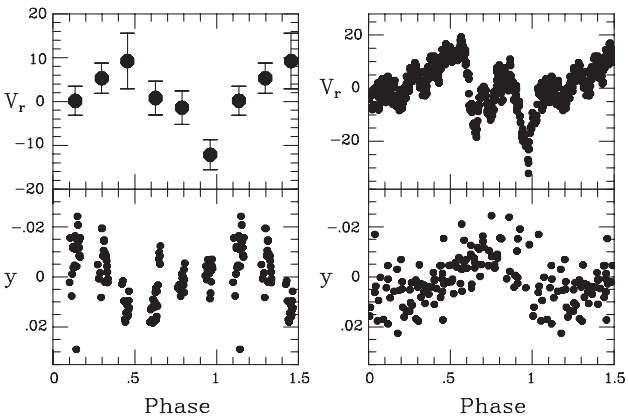

Figure 6. Left-hand panel: Strömgren *y* light curve (bottom panel) and radial velocity curve (top panel) for the $\nu_1 = 0.170\,19\,\mathrm{cycle\,d^{-1}}$ frequency. Right-hand panel: the same for the $\nu_2 = 4.889\,56\,\mathrm{cycle\,d^{-1}}$ frequency. The epoch of phase zero is HJD 245 1900.0840.

calculated in this way for ν_1 and ν_2. It is interesting to note that in both the ν_0 and ν_2 radial velocity curves, there is a discontinuity in the falling branch. This phenomenon is visible in other β Cep stars with high amplitude, such as BW Vul (Mathias et al. 1998) and is interpreted in terms of a shock wave. In this case, however, there is another explanation (see below).

5 MODE IDENTIFICATION OF ν_0 USING PHOTOMETRY

It is well known that the relative light amplitudes and phases depend on the spherical harmonic degree, ℓ, but are independent of m (Stamford & Watson 1981). From the relative amplitudes and phases at two passbands, it is possible to construct regions for various values of ℓ in the relative amplitude versus phase difference diagram. In constructing these regions, the non-adiabacity parameter, R, and phase, ψ, is given all possible values. In Heynderickx et al. (1994), ψ was fixed to 180° and R adjusted for a best fit with observations for each chosen value of ℓ. However, it is possible to calculate R and ψ from linear, non-adiabatic pulsation models, which should be reasonably reliable for B-type stars where convective transport can be neglected. Balona & Evers (1999) used such models in mode identification for some δ Scuti stars.

We used Dziembowski's NADROT code applied to stellar models calculated using the Warsaw–New Jersey evolutionary code. For each eigenmode, the real, $f_{\rm R}$, and imaginary, $f_{\rm I}$, parts of the temperature-to-radius eigenfunction ratio are calculated. These values are directly related to R and ψ, and can be used to increase the discrimination between various values of ℓ.

As 19 Mon is a rapid rotator, the observed frequency is greatly affected by the rotational frequency, Ω. To obtain the approximate frequency in the absence of rotation, the quantity $m\Omega$ needs to be added to the observed frequency. From Section 3 we estimate $0.7 < \Omega < 1.4\,{\rm cycle\,d^{-1}}$. NADROT calculates the unstable eigenfrequencies in a non-rotating star, giving the value of ℓ, frequency and $f_{\rm R}$ and $f_{\rm I}$. We can compare each calculated frequency with the ν_0 frequency in 19 Mon adjusted for a non-rotating star using values of m such that $-m \le \ell \le m$ and the range of Ω mentioned above. Using models with masses between 12 and $16\,{\rm M}_\odot$, we considered the match a satisfactory one if the difference between the calculated frequency and the corrected value of ν_0 differed by less than $0.25\,{\rm cycle\,d^{-1}}$.

Most of the matching frequencies are $(2,-2)$, $(1,-1)$ or $(2,-1)$ modes. With the values of $f_{\rm R}$ and $f_{\rm I}$ obtained for these matching frequencies, we were able to calculate the relative amplitudes and phase differences. Fig. 7 shows the regions predicted for various values of ℓ as well as the actual ratios and phase differences, with respect to the u band, for the *uvby* data. While there is some overlap between $\ell = 1$ and 2, the results are consistent with the $\ell = 2$ identification proposed by Heynderickx et al. (1994).

Although Fig. 7 shows that the most probable value is $\ell = 2$ or, possibly, $\ell = 1$, it is not an entirely satisfactory method of mode identification. To make full use of the information in the photometry one must set up a criterion, which minimizes the differences between the observed and predicted amplitude ratios and phase differences. This method was developed by Balona & Evers (1999). Using the same criterion for matching of the calculated frequency and the corrected value of ν_0, we can calculate a goodness-of-fit criterion for matching of amplitude ratios and phase differences in all four colours as described in Balona & Evers (1999). This allows us to attach a probability, p, of correct mode identification for any given match. The results are summarized in Fig. 8. The figure shows histograms of the probability for modes with $\ell = 0$, 1 and 2. It is evident that $\ell = 2$ modes give a better fit to the data than $\ell = 1$. The highest probability for $\ell = 2$ is $p = 0.89$, for $\ell = 1$ it is $p = 0.72$ and for $\ell = 0$ it is $p = 0.47$. The probability that ν_0 is a radial mode can therefore be safely excluded.

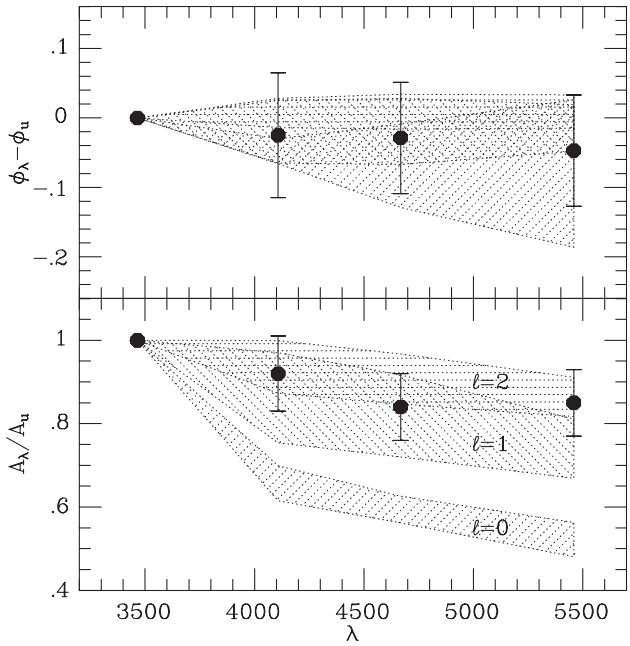

Figure 7. Amplitude ratios (bottom panel) and phase differences (top panel) relative to the Strömgren u band. The solid filled circles are the observations. The hatched areas give the expected positions for $\ell = 0$, 1 and 2.

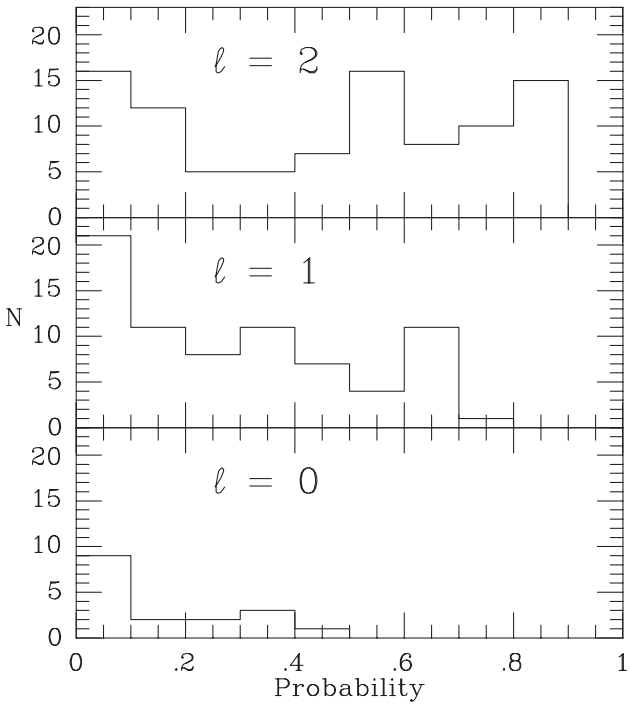

Figure 8. The number of modes, N, which match the observed photometric amplitudes and phases for frequency ν_0 is shown as a function of probability of the match for various values of ℓ. Modes were calculated using a non-adiabatic pulsation code.

6 LINE PROFILE VARIATIONS

The radial velocities only give information concerning the core of the line profile. To obtain a complete picture of the line profile variations, one needs to study the variations over the whole profile. The most convenient way of doing this is to construct 'difference profiles' by dividing each line profile by the mean line profile from all the observations. In this way, even small departures from the mean line profile can be visualized in a grey-scale diagram. By stacking difference spectra as a function of time in such a diagram, the variation of the line profiles with time can be easily seen.

Instead of analysing just a single spectral line in this way, the noise level can be lowered by simultaneous use of many lines. This can be achieved by cross-correlating an unbroadened synthetic spectrum with the observed spectrum. The resulting correlation function is essentially a weighted mean of the absorption lines sampled by the synthetic spectrum. To do this we used the SPECTRUM program (Gray & Corbally 1994) to produce an unbroadened spectrum of a star with $T_{\rm eff} = 24\,000$ and $\log g = 3.50$. We masked out orders containing telluric lines and the Balmer lines. The resulting correlation functions show distinct moving subfeatures, which are best seen in the grey-scale plots of Fig. 9.

The reason for the discontinuity around zero phase in the radial velocity curves of Fig. 5 is now clear. The line profile variations consist of two moving absorption subfeatures. As they pass through the centre of the line profile, the radial velocity is determined from the core of one feature and suddenly switches to the core of the other feature as it gains in absorption depth at the expense of the first one. The centroid variation is free of this effect. While this provides the explanation in the case of 19 Mon, it is unlikely that it holds in the case of other stars such as BW Vul, which seem to be pulsating in the radial mode.

As can be seen from Fig. 9, the main pulsation, ν_0, gives rises to two absorption subfeatures, which move from blue to red, suggesting a prograde ($\ell = 2, m = -2$) mode. Note that there is a fair amount of detail in the absorption subfeatures. This could be a result of interference by modes of higher degree but close to ν_0 in frequency. In Fig. 10 we show grey-scale plots of the data phased with ν_0 for the SAAO and MSSSO spectra.

It is clear from the grey-scale figures that ν_0 is a prograde non-radial mode, the two moving absorption subfeatures indicate $\ell = 2, m = -2$, in agreement with the photometric mode identification. It would be interesting to calculate the pulsation parameters that best describe the line profile variations for ν_0. There are only two methods that are capable of doing this: the method of moments developed by Balona (1987) and refined by Aerts, De Pauw & Waelkens (1992) and the direct fitting method first developed by Balona & Kambe (1999).

The direct fitting method simply searches for the best pulsational parameters that fit the line profiles for a given period. In general, there are five free parameters for any given mode (ℓ, m): the angle of inclination, i, the vertical pulsational amplitude, $V_{\rm p}$, and pulsational phase, $\phi_{\rm p}$, and the pseudo-velocity amplitude, $V_{\rm f}$, and phase, $\phi_{\rm f}$, owing to the coupling between temperature variations and rotation. To apply the method, we first find the mean line profile at several phases during the pulsation cycle. If there are sufficient line profiles, the variations owing to other modes should cancel out when forming the mean line profile at a given phase. Next, for a fixed value of (ℓ, m) we vary the parameters and calculate the goodness of fit. The most likely parameters are those

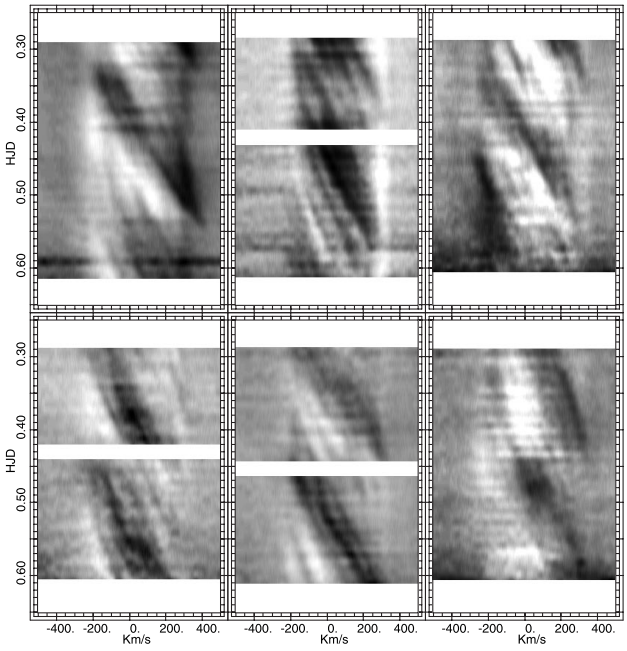

Figure 9. Nightly grey-scale plots of residual profiles. Bottom panel, left to right: HJD 245 1917, 245 1918, 245 1919. Top panel, left to right: HJD 245 1921, 245 1924, 245 1925. Black areas represent extra absorption.

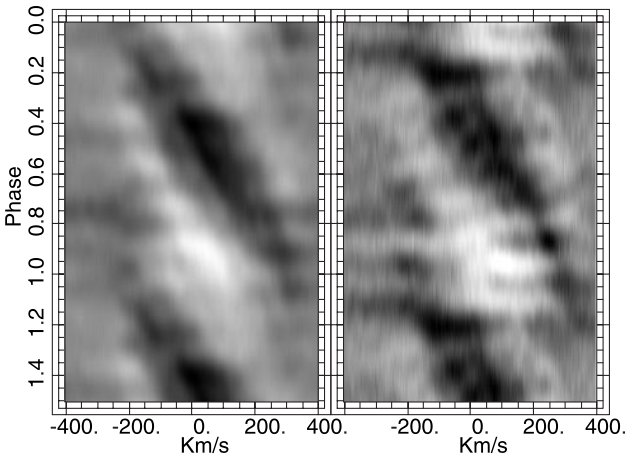

Figure 10. Grey-scale plots of all SAAO (left) and MSSSO (right) residual profiles phased with $\nu_0 = 5.23\,{\rm cycle\,d^{-1}}$.

that minimize the fitting error. We assume that the eigenfunction can be represented by a single spherical harmonic (ℓ, m), which is a good approximation for ν_0 because the pulsation period is much shorter than the period of rotation ($\Omega/\nu_0 \approx 0.2$).

Because the line profile variations caused by temperature are not well decoupled from those caused by pulsation, a solution for all five parameters will probably not give the best results. We can use results of linear non-adiabatic pulsation models to calculate $f_{\rm R}$ and $f_{\rm I}$ and use these values to fix the ratio $V_{\rm f}/V_{\rm p}$. It is easy to show that

$$\frac{V_{\rm f}}{V_{\rm p}} = \frac{v \sin i}{\omega_0 r}\left[\left(\frac{1}{4}\alpha_T f_{\rm R} + \alpha_{\rm g} C_1\right)^2 + \left(\frac{1}{4}\alpha_T f_{\rm I}\right)^2\right]^{1/2}$$

(Balona 2000), where ω_0 is the angular frequency of pulsation in

Table 4. Results of the direct-fitting technique applied to the ν_0 periodicity adopting $V_f/V_p = 0.45$. For each mode, (ℓ, m), we give the angle of inclination, i (degrees), the phase of the flux variation, ϕ_f (in periods), vertical pulsational amplitude, V_p (km s^{-1}) and phase, ϕ_p (in periods) and the variance of the fit, σ, in arbitrary units. Phases are with respect to HJD 245 1900.084, the time of maximum light.

(ℓ, m)	i	ϕ_f	V_p	ϕ_p	σ
(2, −1)	29	0.427	28	0.564	2.600
(2, −2)	38	0.220	31	0.013	2.623
(3, −2)	48	0.212	24	0.030	2.720
(1, −1)	39	0.180	48	0.576	2.731
(3, −3)	39	0.475	24	0.557	2.761
(4, −2)	27	0.394	23	0.036	2.949
(3, −1)	35	0.498	27	0.553	3.034
(4, −4)	48	0.200	16	0.034	3.096
(4, −3)	32	0.433	15	0.554	3.139
(1,0)	37	0.534	29	0.549	3.752
(0,0)	90	0.532	38	0.570	3.796
(2,0)	37	0.535	29	0.550	3.915
(4, −1)	32	0.480	20	0.550	4.072
(3,0)	45	0.562	29	0.537	4.109
(2,1)	27	0.549	28	0.533	4.480
(4,0)	50	0.543	29	0.538	4.526
(3,1)	27	0.530	17	0.554	4.611
(4,1)	28	0.567	13	0.565	4.965
(1,1)	90	0.022	15	0.021	5.454
(2,2)	27	0.603	5	0.632	5.596
(3,3)	28	0.407	6	0.518	5.629
(3,2)	79	0.000	15	0.050	5.653
(4,3)	89	0.809	16	0.010	5.676
(4,2)	69	0.002	10	0.014	5.681
(4,4)	32	0.001	5	0.010	5.696

the absence of rotation and r is the stellar radius. The quantities

$$\alpha_T = \left(\frac{\partial \log F_\lambda}{\partial \log T_{\rm eff}}\right)_{\rm g} \quad \text{and} \quad \alpha_{\rm g} = \left(\frac{\partial \log F_\lambda}{\partial \log g}\right)_{T_{\rm eff}}$$

can be obtained from a model atmosphere. From a Kurucz model appropriate to 19 Mon, we obtain $\alpha_T = 1.90, \alpha_g = -0.027$ with only a slight dependence on wavelength over the visible region. Because f_R and f_I depend on mode and frequency, we need to know the frequency that the mode would have in the non-rotating case. We used the procedure described in the previous section to pick out the modes from the models that are most likely correspond to ν_0. For every mode matched in this way, we used the above equation to calculate V_f/V_p. We find that the mean value is $\langle V_f/V_p\rangle = 0.45 \pm 0.01$ for all unstable modes with $0 < \ell < 3$, though the range is quite large (0.32–0.78).

Next, we calculated the mean line profile, as obtained by cross-correlation, at 20 phases. A first pass was made in which V_f/V_p was fixed at 0.45, V_p was allowed to take values from 0 to 50 km s^{-1} in steps of 5 km s^{-1}, ϕ_f and ϕ_r took values from 0 to 1 periods in steps of 0.2 periods and the angle of inclination, i, was varied from 40° to 90° in steps of 5°. The projected rotational velocity was fixed at 275 km s^{-1} and the intrinsic line profile was assumed to be a Gaussian with width 18 km s^{-1}, which is the typical rms linewidth of the intrinsic line profile calculated from the SPECTRUM code. Fits were made for all values of ℓ and m from $\ell = 0$ to 4 using the part of the profile within 200 km s^{-1} of the line centre. These calculations allowed a global minimum to be found in the standard error of the fit to the observed profiles. With these parameters as starting values, we can then improve the fit. The results shown in Table 4 indicate that $(2, -1)$ or $(2, -2)$ give the best results. However, the angle of inclination for $(2, -1)$ implies that the star is rotating at greater than critical rotational velocity.

Table 5. As in Table 4, but holding $V_f/V_p = 0.45$ and $i = 80°$ fixed.

(ℓ, m)	ϕ_f	V_p	ϕ_p	σ
(2, −2)	0.172	20	0.028	2.638
(3, −3)	0.400	16	0.567	2.822
(1, −1)	0.401	30	0.585	2.992
(3, −2)	0.001	54	0.039	3.203
(4, −4)	0.211	11	0.028	3.253
(2, −1)	0.472	74	0.549	3.443
(4, −3)	0.400	40	0.543	3.713
(0,0)	0.528	35	0.568	3.827
(3,0)	0.579	69	0.525	4.665
(1,0)	0.537	55	0.550	4.678
(4, −2)	0.040	36	0.010	4.797
(4, −1)	0.496	49	0.534	4.873
(3, −1)	0.502	47	0.554	5.032
(1,1)	0.006	16	0.011	5.492
(3,1)	0.001	47	0.999	5.590
(4,1)	0.998	15	0.052	5.590
(2,0)	0.010	30	0.390	5.616
(4,0)	0.004	14	0.211	5.652
(2,1)	0.005	10	0.825	5.666
(3,2)	0.005	15	0.001	5.668
(4,2)	0.002	3	0.028	5.690
(4,3)	0.601	10	0.611	5.729
(3,3)	0.932	0	0.728	5.737
(2,2)	0.623	0	0.198	5.739
(4,4)	0.600	0	0.200	5.750

Allowing the angle of inclination, i, to vary is probably not a good idea because there is a coupling between i and other pulsational parameters. We know that $i > 30°$ (see Section 3). Performing the same solutions, but holding the angle of inclination fixed at $i = 80°$ gives the results shown in Table 5. This time $(2, -2)$ gives the best fit. Fixing i at $i = 60°$ also gives $(2, -2)$ as the best-fitting mode.

Given (ℓ, m) and the pulsational parameters, it is possible to calculate the light amplitude. The result depends on the adopted rotational frequency, Ω, which is not well known. Using the parameters of $(2, -2)$ from Table 5 we calculate that the light amplitude in y should be 0.03 mag if $\Omega = 0.7$ and 0.05 mag if $\Omega = 1.4$. The phasing of the light curve agrees quite closely (within 0.1 periods) with observations, but the observed amplitude is smaller at 0.02 mag (Table 2). One could adjust the values of the non-adiabatic constants f_R and f_I to reproduce the observations exactly. Considering the uncertainties of the model, we do not believe this is justified. Reasonable agreement is obtained with the smallest value of Ω, implying that the angle of inclination is quite close to 90°.

In Fig. 11 we show grey-scale plots of the correlation line profiles folded with frequencies $\nu = 1.17$ and $\nu_2 = 4.89$ cycle d^{-1}. The first frequency is the 1-d alias of ν_1; we could not obtain a meaningful grey-scale image of ν_2 because of interference from ν_0 and significant gaps in phase coverage. The figure suggest that both periodicities could also be prograde $m = -2$ modes. Neither frequency is detected with significant in our *uvby* data, but a force fit gives the parameters shown in Table 6.

We applied the direct fitting technique to ν_2 adopting $V_f/V_p = 0.45$ and $i = 80°$. Results are shown in Table 7. The discrimination between various modes is not as clear as for ν_0, but it

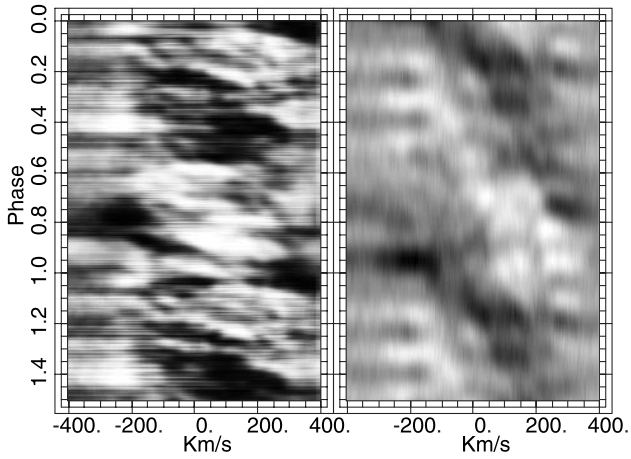

Figure 11. Grey-scale plots of the correlation line profiles phased with $\nu = 1.170\,19\,\mathrm{cycle\,d^{-1}}$ (left-hand panel) and $\nu_2 = 4.889\,56\,\mathrm{cycle\,d^{-1}}$ (right-hand panel).

Table 6. Amplitudes and phases of the three periodic components in 19 Mon. Amplitudes are in mag or $\mathrm{km\,s^{-1}}$ and phases are in radians with respect to HJD 245 1900.084.

Quantity	Amplitude	Phase
ν_0:		
y	0.023 ± 0.001	0.00 ± 0.05
b	0.022 ± 0.001	0.01 ± 0.05
v	0.025 ± 0.002	0.09 ± 0.06
u	0.026 ± 0.002	0.07 ± 0.06
Singlets	30 ± 2	0.36 ± 0.07
Triplets	30 ± 3	3.84 ± 0.09
Balmer	20 ± 3	3.83 ± 0.07
ν_1:		
y	0.009 ± 0.001	5.40 ± 0.13
b	0.009 ± 0.001	5.45 ± 0.13
v	0.008 ± 0.002	5.44 ± 0.20
u	0.011 ± 0.002	5.33 ± 0.16
Singlets	8 ± 3	4.72 ± 0.26
Triplets	12 ± 3	5.48 ± 0.25
Balmer	1 ± 1	2.59 ± 1.00
ν_2:		
y	0.009 ± 0.001	1.59 ± 0.13
b	0.010 ± 0.001	1.58 ± 0.11
v	0.010 ± 0.002	1.75 ± 0.17
u	0.013 ± 0.002	1.60 ± 0.13
Singlets	8 ± 2	5.77 ± 0.28
Triplets	11 ± 3	3.47 ± 0.26
Balmer	4 ± 1	3.74 ± 0.44

seems that ν_2 is probably a mode with $\ell = 1, m = -1$ or $\ell = 2, m = -2$.

The nature of the low frequency $\nu_1 = 0.17\,\mathrm{cycle\,d^{-1}}$ is uncertain. If this is indeed the true frequency, rather than one of its 1-d aliases at 0.83 or $1.17\,\mathrm{cycle\,d^{-1}}$, it is unlikely to be due to rotation because the implied rotational period of nearly 6 d seems too long (see Section 3). There is no evidence of binary motion from the radial velocities, so we conclude that it is most probably pulsational in nature. However, the star is outside the instability strip for SPB stars (Fig. 12). We did not try to identify the mode ν_2 because the light amplitude is too small and not visible in the periodogram of our *uvby* data.

Table 7. Results of direct-fitting technique applied to the ν_2 periodicity adopting $V_f/V_p = 0.45$. For each mode, (ℓ, m), we give the phase of the flux variation, ϕ_f (in periods), vertical pulsational amplitude, V_p ($\mathrm{km\,s^{-1}}$) and phase, ϕ_p (in periods) and the variance of the fit, σ, in arbitrary units. Phases are with respect to HJD 245 1900.084.

(ℓ, m)	ϕ_f	V_p	ϕ_p	σ
(1, −1)	0.894	11	0.913	2.486
(2, −2)	0.804	10	0.399	2.563
(0,0)	0.944	18	0.950	2.577
(2, −1)	0.953	27	0.940	2.602
(1,0)	0.025	34	0.905	2.672
(3, −3)	0.765	6	0.948	2.686
(3, −2)	0.380	21	0.413	2.748
(4, −4)	0.921	5	0.410	2.793
(2,0)	0.800	21	0.396	2.817
(4,0)	0.405	24	0.411	2.831
(1,1)	0.421	9	0.410	2.851
(3, −1)	0.991	16	0.415	2.879
(3,0)	0.856	24	0.000	2.884
(3,1)	0.407	15	0.625	2.892
(4, −1)	0.978	14	0.898	2.920
(4, −3)	0.796	11	0.000	2.922
(4,1)	0.410	20	0.404	2.925
(4,2)	0.384	11	0.390	2.928
(2,1)	0.865	5	0.381	2.937
(4, −2)	0.601	15	0.201	2.952
(3,2)	0.402	5	0.001	2.967
(2,2)	0.201	5	0.010	2.971
(4,3)	0.614	5	0.595	2.982
(4,4)	0.994	0	0.988	2.997
(3,3)	0.997	0	0.998	3.002

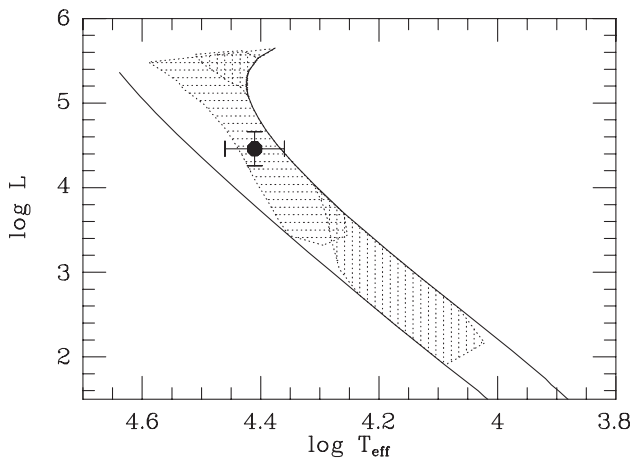

Figure 12. Location of 19 Mon in the Hertzsprung–Russell diagram. The horizontally hatched region is the theoretical location of the unstable $\ell = 2$ region for β Cep stars (short-period modes) while the vertically hatched region is the theoretical location for SPB stars.

7 CONCLUSIONS

As the evidence for Hα emission is marginal, it is not clear whether 19 Mon can really be considered as a Be star. Certainly, there are no indications of Hα emission or even a reduction of line strength. The EW of Hα in our observations is normal for a star of this type. It occurred to us that the perceived emission could perhaps occur at certain phases when the absorption subfeatures are placed

symmetrically on the line wing, which occurs close to the time of light maximum. We tested this idea by looking at the Hα line profile at the appropriate phase range. Our impression is that the presence of telluric lines of variable intensity has a much larger effect on the appearance of the line core than the pulsation. In Hβ and Hγ, which are free of telluric lines, no obvious line doubling is seen, though the distortion caused by the moving absorption subfeatures is visible. We conclude that the classification of 19 Mon as a Be star could not have been influenced by the pulsation unless, of course, the pulsation had a much larger amplitude at that time.

Our observations of 19 Mon show that three periodicities are present: $\nu_0 = 5.229\,94\,\mathrm{cycle\,d^{-1}}$, $\nu_1 = 0.170\,19\,\mathrm{cycle\,d^{-1}}$ and $\nu_2 = 4.889\,56\,\mathrm{cycle\,d^{-1}}$. While ν_0 and ν_2 can only be understood as being owing to pulsation, the nature of ν_1 is a puzzle because no unstable modes exist at this period in models of the star. It is possible that it could be a prograde sectorial mode shifted to low frequencies due to rotation and which would have a much higher frequency in a non-rotating star. The possibility also exists that one of the two daily aliases of ν_1 might be the true periodicity, in which case a rotational effect could be invoked.

It is quite clear from profile fitting that ν_0 is a quadrupole prograde mode, $\ell = 2, m = -2$. This identification agrees with the relative amplitudes and phases of the observed *uvby* light curves and also predicts approximately the right amplitudes and phases. The most serious obstacle in obtaining asteroseismological information from the star is the unknown rotational period of the star.

Although 19 Mon was originally selected on the basis that it has been classified as a marginal Be star, the Be nature of the star is not supported by our observations. It should perhaps be considered as a non-Be star until such time as the emission, if it is present, is more apparent in the spectrum.

ACKNOWLEDGMENTS

LAB would like to thank W. A. Dziembowski for the use of NADROT and A. Pamyatnykh for the Warsaw–New Jersey evolution code. DJJ thanks the British Particle Physics and Astronomy Research Council for a post-doctoral research fellowship, and the Royal Society for a European research grant. DJJ would like to acknowledge the continued positive influences of Mrs J Pryer.

REFERENCES

Aerts C., De Pauw M., Waelkens C., 1992, A&A, 266, 294
Balona L. A., 1977, MemRAS, 84, 101
Balona L. A., 1987, MNRAS, 224, 41
Balona L. A., 1990, MNRAS, 245, 92
Balona L. A., 1994, MNRAS, 268, 119
Balona L. A., 1995, MNRAS, 277, 1547
Balona L. A., 2000, in Breger M., Montgomery M. H., eds, ASP Conf. Ser. Vol. 210, Delta Scuti and Related Stars. Astron. Soc. Pac., San Francisco, p. 170
Balona L. A., Crampton D., 1974, MNRAS, 166, 203
Balona L. A., Cuypers J., Marang F., 1992, A&AS, 92, 533
Balona L. A., Engelbrecht C., 1979, MNRAS, 189, 171
Balona L. A., Evers E. A., 1999, MNRAS, 302, 349
Balona L. A., Kambe E., 1999, MNRAS, 308, 1117
Balona L. A., Krisciunas K., 1994, IBVS, 4022
Balona L. A., Rozowsky J., 1991, MNRAS, 251, 66P
Balona L. A., Shobbrook R. R., 1984, MNRAS, 211, 375
Gray R. O., Corbally C. J., 1994, AJ, 107, 742
Heynderickx D., 1992, A&AS, 96, 207
Heynderickx D., Waelkens C., Smeyers P., 1994, A&AS, 105, 447
Hirata R., Asada Y., 1976, PASJ, 28, 713
Irvine N. J., 1975, ApJ, 196, 773
Mathias P., Gillet D., Fokin A. B., Cambon T., 1998, A&A, 339, 525
Slettebak A., 1982, ApJS, 50, 55
Slettebak A., Howard R. F., 1955, ApJ, 121, 102
Stamford P. A., Watson R. D., 1981, Ap&SS, 77, 131

This paper has been typeset from a TEX/LATEX file prepared by the author.